Biogeosciences Discuss., 7, 745–764, 2010
www.biogeosciences-discuss.net/7/745/2010/

Biogeosciences Discussions

This discussion paper is/has been under review for the journal Biogeosciences (BG).
Please refer to the corresponding final paper in BG if available.

A mechanistic account of increasing seasonal variations in the rate of ocean uptake of anthropogenic carbon

T. Gorgues[1], **O. Aumont**[2], **and K. B. Rodgers**[3]

[1]Institut Universitaire Européen de la Mer (UMS3113), CNRS, centre IRD de Bretagne, Plouzané, France
[2]Laboratoire de Physique des Océans (UMR6523), IRD, centre IRD de Bretagne, Plouzané, France
[3]Atmospheric and Ocean Sciences, Princeton University, Princeton, New Jersey, USA

Received: 9 January 2010 – Accepted: 15 January 2010 – Published: 29 January 2010

Correspondence to: T. Gorgues (thomas.gorgues@ifremer.fr)

Published by Copernicus Publications on behalf of the European Geosciences Union.

Abstract

A three-dimensional circulation model that includes a representation of anthropogenic carbon as a passive tracer is forced with climatological surface fluxes. This simulation is then used to compute offline the anthropogenic ΔpCO_2 (defined as the difference between the atmospheric CO_2 and its seawater partial pressure) trends over three decades between the years 1970 and 2000. It is shown that the mean increasing trends in ΔpCO_2 reflects an increase of the seasonal amplitude of ΔpCO_2. In particular, the ocean uptake of anthropogenic CO_2 is decreasing (negative trends in ΔpCO_2) in boreal (austral) summer in the Northern (Southern) Hemisphere in the subtropical gyres between 20° N(S) and 40° N(S). In our simulation, the increased amplitude of the seasonal trends of the ΔpCO_2 is mainly explained by the seasonal sea surface temperature (SST) acting on the anthropogenic increase of the dissolved inorganic carbon (DIC). It is also shown that the seasonality of the anthropogenic DIC has very little effect on the decadal trends. This study underscores the need for surface CO_2 measurements that resolve the seasonal cycle throughout much of the extratropical oceans.

1 Introduction

Currently anthropogenic activities (fossil fuel burning, deforestation and cement production) contribute approximately 7 Pg C of atmospheric CO_2 each year (Marland et al., 2005; IPCC, 2007). Around half of this anthropogenic CO_2 is absorbed by the ocean and the terrestrial biosphere (Battle et al., 2000; Sarmiento et al., 2000; Keeling and Garcia, 2002; Takahashi et al., 2002; Quay et al., 2003; Sabine et al., 2004). The ocean uptake response to the increased atmospheric partial pressure CO_2 (hereafter pCO_{2atm}) has been the focus of a long series of publications (e.g., Sarmiento et al., 1992; Anderson et al., 2002; Takahashi et al., 2002, 2006, 2009; Rodgers et al., 2008). Most of them focus on the mean rates of change in the ocean uptake of

BGD

7, 745–764, 2010

atmospheric CO_2 and use annual means for the partial pressure of CO_2 in seawater (hereafter pCO_{2sw}) or assume that its seasonal cycle remains unchanged (Takahashi et al., 2006). But data-based studies in the North Atlantic have shown that the pCO_{2sw} increases more rapidly in boreal summer than in winter, challenging this assumption (Lefèvre et al., 2004; Schuster and Watson, 2007). In these studies, hypotheses for the North Atlantic involving declining biological productivity (Lefèvre et al., 2004) or winter-time mixing and reduced buffer capacity (Schuster and Watson, 2007) have been offered to explain the decreasing ΔpCO_2 trends in boreal summer. The modeling study of Rodgers et al. (2008) identified seasonal changes in ΔpCO_2 (here defined as the difference between pCO_{2atm} and pCO_{2sw}) as accounting for an important component of decadal changes in the North Pacific. However, as the reanalysis fluxes used to force the ocean model in that study included variations on all timescales (storms to decadal), it was not possible there to identify quantitatively specifically the seasonal effect. For that reason, we have chosen here an experimental design where the physical forcing consists of a repeating seasonal cycle over the period of the anthropogenic transient in atmospheric CO_2 concentration. This allows for a focus specifically on the way in which the anthropogenic transient signal may project itself onto the seasonal cycle in ocean surface conditions.

The primary aim of this present work is to assess the different processes responsible for the decadal trends of the anthropogenic ΔpCO_2 over the global ocean. A parallel aim of this study is to test the hypothesis that an ocean observing network that does not resolve the seasonal cycle in surface ocean pCO_2 will result in significant biases in the rate of uptake of CO_2 by the ocean. After briefly presenting our method and describing the mean decadal trends in anthropogenic ΔpCO_2, our study will focus on the seasonality of these trends. Finally, the processes influencing these trends will be discussed.

2 Method

The model configuration considered here consists of a dynamical ocean-ice model, and a passive tracer module for the anthropogenic carbon perturbation that is run offline using output from the dynamical model. The dynamical component is the ORCA2-LIM global coupled ocean-ice model that is based on Version 9 of OPA (Océan PArallélisé). OPA is a finite difference model with a free surface and a nonlinear equation of state following the formulation of Jackett and McDougall (1995) (Madec and Imbard, 1996; Madec et al., 1998). The domain is global and extends from 78° S to 90° N. The bottom topography and coastlines are derived from the study of Smith and Sandwell (1997), complemented by the ETOPO5 data set. Lateral mixing is oriented isopycnally, and the eddy parameterization scheme of Gent and McWilliams (1990) is applied poleward of 10°. Vertical mixing is achieved using the TKE scheme of Blanke and Delecluse (1993).

For the ORCA2 grid configuration, the zonal resolution is 2°, and meridional resolution ranges from 0.5° at the equator to 2° toward the poles. The model grid is tripolar, with two poles in the Northern Hemisphere (over North America and Siberia) and one centered over Antarctica. The model uses 31 layers in the vertical, with 20 of these layers lying in the upper 500 m. The ocean model is coupled to a sea ice model (Fichefet and Maqueda, 1997; Goosse and Fichefet, 1999). The model was initialized with Boyer et al. (1998) and Antonov et al. (1998) salinity and temperature climatologies. It was then spun up for 100 yr with surface momentum forcing fields from a daily mean climatology of wind stress from the ERA40 reanalysis (Uppala et al., 2005).

In this study, only the anthropogenic perturbation of DIC (DIC_{ant}) and pCO_{2sw} is computed offline using five-day mean circulation fields from the last year of the 100-year spin-up of a circulation model. This representation of the anthropogenic perturbation assumes that the natural (pre-anthropogenic) carbon cycle remained unchanged despite the anthropogenic increase (most importantly, biological fluxes remain stationary in a climatological sense). The anthropogenic air-sea CO_2 fluxes are computed by taking the difference between the carbon fluxes which include the simulated perturbation

BGD
7, 745–764, 2010

and the natural carbon fluxes. The latter is inferred by reading monthly mean DIC and alkalinity surface fields as provided from a climatological experiment using PISCES as described in Aumont and Bopp, (2006). The control simulation (hereafter DELC) has been forced by the atmospheric CO_2 concentration from 1860 to 2000. The carbonate chemistry follows the OCMIP protocols (see the OCMIP website for more information at www.ipsl.jussieu.fr/OCMIP) and the gas exchange coefficient is computed from the relationship of Wanninkhof (1992).

In order to identify the relative impacts of seasonal variations of DIC, SST, Alkalinity and Salinity on the ΔpCO_2 trends, we also performed a series of perturbate calculations using monthly and annual mean surface fields from the fully three-dimensional model. The anthropogenic partial pressure of carbon dioxide in the ocean's surface waters ($pCO_{2sw,ant}$) is determined by following the protocols of DOE (1994) from dissolved inorganic carbon (DIC), alkalinity, and the dissociation constants of carbonic acid. Using these perturbation calculations, we have decoupled the different processes responsible for the anthropogenic ΔpCO_2 trends in the global ocean.

3 Results

The annual mean linear trend in ΔpCO_2 over the period 1970–2000 reveals an increase over most of the global ocean (Fig. 1), except for local signals along the Arctic coast of Russia and in Hudson Bay. Positive values indicate regions where the pCO_{2sw} lags the trend in the atmospheric pCO_2 over 1970–2000. The annual mean pattern also reveals an extensive local minimum in the center of the subtropical gyres in both hemispheres (Fig. 1) where the trend is almost zero. Local minima are also found in the Eastern Bering Sea, the region east of Hokkaido and the region east of Newfoundland (Fig. 1). In the annual mean, significant negative trends only occur along the Arctic coast of Russia and in Hudson Bay. The overall maximum is found along the Antarctic coast due to the ice sheet that shields the ocean from the anthropogenic increase of atmospheric CO_2 and the emergence of water masses with low anthropogenic pCO_2. Local maxima tend to be found along the equatorward and poleward margins of the

subtropical gyres, in the Polar seas, as well as in the Mediterannean. For the North Pacific, the structures here are consistent with the perturbation structures described in Rodgers et al. (2008). For this annual mean representation, the results presented here are also compared with the data analysis presented in the studies of Takahashi et al. (2006, 2009) (Fig. 1). For comparison, we have computed the ΔpCO_2 decadal trends from the pCO_{2sw} trends that were considered in those studies. Those data are not directly comparable to our control simulation. Indeed, there are by construction no decadal changes in the physical state of the ocean for our control simulation over the time-period considered in this study. However, the modeled trends are almost always in the range of the trends computed from the data published in Takahashi et al. (2006, 2009) when uncertainty is taken into account. It also appears that the trends published in Takahashi et al. (2006, 2009) show local minima in the center of the subtropical gyres in the Northern Hemisphere, with this also being consistent with our control simulation.

Figure 2a, b shows the respective decadal trends of sea surface ΔpCO_2 for February and August considered separately over 1970–2000. In February, the Northern Hemisphere displays the same overall pattern (Fig. 2a) seen in the annual mean trend (Fig. 1), with less pronounced minima in the subtropical gyres. Additionally, the negative decadal trend that was found near the Arctic coast of Russia and in Hudson Bay for the annual mean analysis is more pronounced in February. In the Southern Hemisphere, the subtropical local minima in February are more pronounced than in the annual mean case.

In August, the Northern Hemisphere summer displays negative ΔpCO_2 trends in the subtropical gyres for both the Pacific and Atlantic basins (Fig. 2b). The minima in the ΔpCO_2 trends east of Hokkaido and Newfoundland become slightly negative as well as for the Eastern Bering Sea and the Japan Sea. On the other hand, the ΔpCO_2 trends associated with the anthropogenic transient increase in the Arctic coast of Russia and the Hudson Bay. In the Southern Hemisphere, the patterns are very similar to those already depicted for the annual mean (Fig. 1) but with less pronounced minima in the subtropical gyre (Fig. 2b).

The decadal trend towards an increased mean annual uptake of anthropogenic CO_2 over the period 1970–2000 (Fig. 1) is then the result of a global increase of the anthropogenic ΔpCO_2 maximum in winter (boreal in the Northern Hemisphere and austral in the Southern Hemisphere) offsetting a slight decrease of the ΔpCO_2 in summer (boreal in the Northern Hemisphere and austral in the Southern Hemisphere) (Fig. 2a, b). Thus, the mean annual increased uptake of anthropogenic CO_2 is in fact accompanied by an increase in the seasonal variability of the ΔpCO_2.

With this analysis of decadal ΔpCO_2 trends for winter and summer seasons considered separately for a repeating seasonal cycle in the physical state of the ocean, the most surprising aspect is that pCO_{2sw} in the subtropical gyres and in the Northern Hemisphere high latitudes tends to increase more rapidly than pCO_{2atm}. Why does this occur? In order to address the underlying mechanism, we performed a series of perturbation calculations. The partial pressure of anthropogenic CO_2 at the ocean surface ($pCO_{2sw,ant}$) is computed using the monthly and annual mean output of modeled DIC, SST, sea surface salinity (SSS) and surface alkalinity using the method prescribed in DOE, (1994). With all fields varying monthly, this perturbation method is able to reproduce well the evolution of ΔpCO_2 obtained with the control simulation (not shown).

In order to identify the relative impacts of seasonal variations in surface DIC concentrations, SST, alkalinity, and salinity on the decadal trends in the seasonal cycle of ΔpCO_2, a series of perturbation calculations were performed where one of these fields was maintained at its annual mean value while the others were allowed to vary seasonally. The resulting decadal ΔpCO_2 trends for February are shown in the first column of Fig. 3, and for August are shown in the second column. The case with annual mean alkalinity is henceforth referred to as MALK, the case with annual mean salinity as MSAL, the case with annual mean DIC as MDIC, and the case with annual mean SST as MSST.

BGD
7, 745–764, 2010

We begin in Fig. 3 with a comparison of both the MALK (Fig. 3a, b) and MSAL (Fig. 3c, d) cases with our control simulation (Fig. 2a, b). In the Northern Hemisphere high latitudes (the Arctic coast of Russia and the Hudson Bay) the MALK case shows a greater amplitude of the seasonal cycles of the ΔpCO_2 trends. At lower latitudes, minima and maxima have a slightly greater amplitude in the MALK computation (Fig. 3a, b) than in MSAL (Fig. 3c, d) or the control simulation DELC (Fig. 2a, b). However, for both of these cases (MALK and MSAL), there is relatively little impact of holding the respective fields to their annual means on the decadal trend in ΔpCO_2 for February or August. This demonstrates that the trends in ΔpCO_2 are not to first order controlled by seasonal variations in either alkalinity or salinity except for the high latitudes in the Northern Hemisphere where alkalinity has a significant impact.

We next consider, respectively the MDIC and MSST cases in Fig. 3e, f and Fig. 3g, h. For these cases, there are distinct differences in the ΔpCO_2 trends for both February and August when they are compared with the distributions seen in Fig. 2a, c. At high latitudes (north of 70° N and south of 50° S), the MDIC case reveals a reversed seasonal cycle with higher trends in winter (boreal for the Northern Hemisphere and austral for the Southern Hemisphere). At lower latitudes, MDIC (Fig. 3e, f) displays higher ΔpCO_2 trends in boreal winter (summer) in the Northern (Southern) Hemisphere. Geographical structures of the trends are also significantly different, with for example no local maxima in the Kuroshio or the Gulf Stream region evident during boreal summer. However, the most striking difference at mid latitudes is an amplified ΔpCO_2 seasonal cycle relative to what is seen in Fig. 2a, b. Negative trends in the North Pacific subtropical gyre reach $-4\,\mu atm\,decade^{-1}$ (vs. $-2\,\mu atm\,decade^{-1}$ in DELC) when positive trends in boreal winter reach $5\,\mu atm\,decade^{-1}$ (vs. $3\,\mu atm\,decade^{-1}$ in DELC).

MSST (Fig. 3g, h) displays, at high latitudes (north of 70° N and south of 50° S), a very similar to DELC (Fig. 2a, b) seasonal cycle of the trends in ΔpCO_2. However at lower latitudes, MSST reveals more dramatic differences with the control simulation DELC. The seasonal cycle is reversed relative to DELC with Northern (Southern) Hemisphere lower trends in ΔpCO_2 occurring in February (August).

This indicates that: i) the significant decadal trends in February and August ΔpCO_2 evident in Fig. 2 in the Northern Hemisphere high latitudes are mostly due to seasonal variations in DIC with the somewhat compensating effects of the alkalinity, ii) at lower latitudes, the seasonal decadal trends are due to the compensating effects of the seasonal variation in SST and DIC. DIC variations, on one end, alkalinity and SST variations, on the other end, tend to act in opposite senses in their modulation of the decadal trends for the different seasons, such that the large impacts of each of these are partially compensating.

4 Discussion

The global-scale response of the decadal ΔpCO_2 trends for the surface ocean to the increased anthropogenic atmospheric CO_2 varies geographically (Fig. 1) and also seasonally (Fig. 2a, b). A comparison of the control run (DELC) with the offline perturbation runs (MALK, MSAL, MDIC, and MSST) clearly demonstrated the first-order importance of the partially compensating effects of SST, alkalinity and DIC to controlling the seasonal trends in ΔpCO_2 seen in Fig. 2. In particular, the summertime trend in the subtropics for pCO_{2sw} to increase more rapidly than atmospheric pCO_2 appears to be driven by seasonal variability in SST since it is opposed by seasonal variations in DIC concentrations and relatively unaffected by seasonality in alkalinity and salinity. Along the Arctic coast of Russia and in Hudson Bay, the seasonal trends are mainly driven by the seasonality of DIC counteracting the seasonality of alkalinity with little effects of the seasonality in salinity and SST.

However, in our simulation and perturbation calculations, by construction there are no decadal trends in surface temperatures or surface alkalinity. The climatological simulation imposed a repeating seasonal cycle in SST and in alkalinity for DELC and the perturbation computations. Thus in the subtropics, seasonal variations in SST alone cannot account for the amplified seasonality in ΔpCO_2 over 1970–2000. Unlike SST,

DIC increases between 1970 and 2000 because of the increase in the CO_{2atm} uptake (Fig. 1). As noted in the results section, the MDIC case shows a significantly stronger increase of the seasonal cycle than the DELC simulation (Fig. 2a, b and Fig. 3e, f). In summer, the increase of DIC and the warm SST induce a year to year increase of pCO_{2sw} which happen to be faster than the increase of CO_{2atm}. The DIC increase has less impact in winter, because SST is colder and the mixed layer deepens bringing waters with low anthropogenic DIC to the surface. The seasonal trends of the anthropogenic ΔpCO_2 in DELC are then the result of the seasonal cycle of SST acting on an increasing DIC concentration.

In the Northern Hemisphere high latitudes, the seasonal variation of the pre-anthropogenic DIC is higher than in most places because the high runoff that peaks in June and decreases the DIC along the Russian coast. The addition of the anthropogenic perturbation of DIC to the seasonal maximum of DIC_{pre} induces a year to year increase of pCO_{2sw} in boreal winter which happens to be faster than the increase of CO_{2atm}.

However, at this stage, the perturbation calculation presented in Fig. 3 does not allow one to distinguish between whether the SST or alkalinity are acting on a mean increase of the DIC seasonal cycle or on a modulation of the seasonal cycle in DIC.

An additional two perturbation calculations have then been performed in order to consider separately the deseasonalized trend in DIC_{ant} and the seasonal component of the evolving DIC_{ant} distribution. This is presented in Fig. 4. For the first case here the pre-anthropogenic component of DIC (DIC_{pre}) was maintained at annual mean values, and the seasonal component of DIC_{ant} was superposed on this (Fig. 4a for February and Fig. 4b for August). For the second case the full seasonal cycle in DIC_{pre} was maintained and the deseasonalized trend in DIC_{ant} was superposed (Fig. 4c for February and Fig. 4d for August). Clearly the first of these two cases (Fig. 4a, b) most closely resemble the MDIC case (Fig. 3e, f). Using the annual mean of the full DIC (preindustrial and anthropogenic as in Fig. 3e, f) and using the annual mean of DIC_{pre} with the seasonal DIC_{ant} does not make any differences (Fig. 4a, b). Figure 4c, d looks very

similar to DELC (Fig. 2a, b). This clearly demonstrates that it is the deseasonalized trend in DIC_{ant} that is acting in conjunction with seasonal variations in SST to drive the amplification of the seasonal cycle in ΔpCO_2 over 1970–2000.

5 Conclusions

Decadal trends in the annual mean of the anthropogenic component of ΔpCO_2 have been shown for a climatologically-forced ocean model to be positive. This is consistent with a tendency towards increased ocean uptake of anthropogenic carbon. However, while the trends of the annual mean values are positive, the seasonal trends simulated in this study show an increase of the amplitude of the seasonal uptake of anthropogenic CO_2 by the ocean in agreement with previous modeling work (Rodgers et al., 2008). In particular, in the Northern (Southern) Hemisphere during boreal (austral) summer, our model displays negative ΔpCO_2 trends in the subtropical gyres. That means that those areas are in fact outgasing anthropogenic carbon in summer. This view is in agreement with the hypothesis of a change in the seasonal cycle of the ocean uptake articulated by Lefèvre et al. (2004).

Our modeling study shows that a possible explanation of this seasonal cycle increase and the subtropical negative trends during summer (boreal in the Northern Hemisphere and austral in the Southern Hemisphere) is the effect of the interplay between seasonal variations in SST and the deseasonalized trend in DIC_{ant}.

In the high latitudes of the Northern Hemisphere, the deseasonalized trend in DIC_{ant} acting on the seasonal cycle of DIC_{pre} is sufficient to explain the negative trends during boreal winter. Seasonal modulation of the DIC_{ant} increase does not affect the ΔpCO_2 trends.

The increase of the anthropogenic CO_2 seasonal cycle of the uptake demonstrated in this study stresses the need of an improved understanding of the processes at play. This study is a first attempt to address this question in a particular configuration with no modification of the ocean circulation or of the ocean biology.

The results considered here have potentially important implications for detection of anthropogenic perturbations in the carbon cycle. Recent studies have suggested that the rate of ocean carbon uptake may be slowing over the North Atlantic as there is a negative decadal trend in ΔpCO_2 (Schuster and Watson, 2007, and references therein). This type of behavior has been attributed to perturbations in the physical climate system, and for the case of the North Atlantic to changes in the state of the Northern Annular Mode. However, we have seen in the control run (where there is no interannual or decadal variability) that sampling that is biased towards summer conditions could result in the inference of a negative trend in ΔpCO_2, even though this trend does not occur in the annual mean. Figure 5 does show that after 30 yr of our simulation, the ΔpCO_2 computed from the boreal winter (summer) trends can differ in the subtropical gyres by almost 10 µatm. Thus although the results here are not intended to provide an interpretation of the specific observations reported by Schuster and Watson (2007), they are intended as a cautionary note regarding the potential importance of aliasing problems with estimates that are reliant on summer data.

The publication of this article is financed by CNRS-INSU.

References

Anderson, L. G. and Olsen, A.: Air-sea flux of anthropogenic carbon dioxide in the North Atlantic, Geophys. Res. Lett., 29(17), doi:10.1029/2002GL014820, 2002.

Antonov, J. I., Levitus, S., Boyer, T. P., Conkright, M. E., O'Brien, T. D., and Stephens, C.: World Ocean Atlas, 1998, Vol. 2, Temperature of the Pacific Ocean, NOAA Atlas NESDIS 28, U.S. Gov. Printing Office, Wash., D.C., 166 pp., 1998.

Aumont, O. and Bopp, L.: Globalizing results from ocean in situ iron fertilization studies, Global Biogeochem. Cy., 20, GB2017, doi:10.1029/2005GB002591, 2006.

Battle, M., Bender, M. L., Tans, P. P., White, J. W. C., Ellis, J. T., Conway, T., Francey, R. J.: Global carbon sinks and their variability inferred from atmospheric O_2 and $\delta^{13}C$, Science, 31, 2467–2470, doi:10.1126/science.287.5462.2467, 2000.

Blanke, B. and Delecluse, P.: Variability of the tropical Atlantic ocean simulated by a general circulation model with two different mixed layer physics, J. Phys. Oceanogr., 23, 1363–1388, 1993.

Boyer, T. P., Levitus, S., Antonov, J., Conkright, M., O'Brien, T., and Stephens, C.: World Ocean Atlas 1998, Vol. 5, Salinity of the Pacific Ocean, NOA Atlas NESDIS 30, 166 pp., US Government Printing Office, Washington, DC, 1998.

DOE: Handbook of Methods for the Analysis of the Various Parameters of the Carbon Dioxide System in Seawater, Version 2, in: ORNL/CDIAC-74, edited by: Dickson, A. G. and Goyet, C., http://cdiac.ornl.gov/oceans/DOE_94.pdf, 1994.

Fichefet, T. and Maqueda, M. M.: Sensitivity of a global sea ice model to the treatment of ice thermodynamics and dynamics, J. Geophys. Res., 102, 12609–12646, 1997.

Gent, P. R. and McWilliams, J. C.: Isopycnal mixing in ocean circulation models, J. Phys. Oceanogr., 20, 150–156, 1990.

Goosse, H. and Fichefet, T.: Importance of ice-ocean interactions for the global ocean circulation: a model study, J. Geophys. Res., 104, 23337–23355, 1999.

Jackett, D. R. and McDougall, T. J.: Minimal adjustment of hydrographic profiles to achieve static stability, J. Atmos. Ocean. Tech., 12, 381–389, 1995.

Keeling, R. F. and Garcia, H. E.: The change in oceanic O_2 inventory associated with recent global warming, P. Natl. Acad. Sci. USA, PNAS, 99(2), 7848-7853, doi:10.1073/pnas.122154899, 2002.

Lefèvre, N., Watson, A. J., Olsen, A., Rios, A. F., and Pérez, F. F.: A decrease in

the sink for atmospheric CO_2 in the North Atlantic, Geophys. Res. Lett., 31, L07306, doi:10.1029/2003GL018957, 2004.
Madec, G. and Imbard, M.: A global ocean mesh to overcome the North Pole singularity, Clim. Dynam., 12, 381–388, 1996.
Madec, G., Delecluse, P., Imbard, M., and Levy, C.: OPA 8.1 general circulation model reference manual, Notes du Pole de Modelisation de l'Institut Pierre-Simon Laplace, 11, 91 pp., http://www.lodyc.jussieu.fr/opa, 1998.
Marland, G. and Boden, T.: Global CO_2 emissions from fossil-fuel burning, cement manufacture, and gas flaring: 1751–2002, Carbon Dioxide Information Analysis Center (CDIAC), Oak Ridge, Tennessee, http://cdiac.esd.ornl.gov/ftp/ndp030/global.1751_2004.ems, 2005.
Quay, P., Sonnerup, R., Westby, T., Stutsman, J., and McNichol, A.: Changes in the $^{13}C/^{12}C$ of dissolved inorganic carbon in the ocean as a tracer of anthropogenic CO_2 uptake, Global Biogeochem Cy., 17(1), 1004, doi:10.1029/2001GB001817, 2003.
Rodgers, K. B., Sarmiento, J. L., Aumont, O., Crevoisier, C., Boyer Montegut, C., and Metzl, N.: A wintertime uptake window for anthropogenic CO_2 in the North Pacific, Global Biogeochemical Cy., 22, GB2020, doi:10.1029/2006GB002920, 2008.
Sabine, C. L., Feely, R. A., Gruber, N., Key, R. M., et al.: The ocean sink for anthropogenic CO_2, Science, 305, 367–371, 2004.
Sarmiento, J. L., Orr, J. C., and Siegenthaler, U.: A perturbation simulation of CO_2 uptake in an ocean general circulation model, J. Geophys. Res., 97, 3621–3645, 1992.
Sarmiento, J. L., Monfray, P., Maier-Reimer, E., Aumont, O., Murnane, R. J., and Orr, J. C.: Sea-air CO_2 fluxes and carbon transport: a comparison of three ocean general circulation models, Global Biogeochem Cy., 14, 1267–1281, 2000.
Schuster, U. and Watson, A. J.: A variable and decreasing sink for atmospheric CO_2 in the North Atlantic, J. Geophys. Res., 112, C11006, doi:10.1029/2006JC003941, 2007.
Smith, W. H. F. and Sandwell, D. T.: Global seafloor topography from satellite altimetry and ship depth soundings, Science, 277, 1957–1962, 1997.
Takahashi, T., Sutherland, S. C., Sweeney, C., Poisson, A., Metzl, N., Tilbrook, B., Bates, N., Wanninkhof, R., Feely, R., Sabine, C., Olafsson, J., and Nojiri, Y.: Global sea-air CO_2 flux based on climatological surface ocean pCO_2, and seasonal biological and temperatude effects, Deep-Sea Res. Pt. II, 49, 1601–1622, 2002.
Takahashi, T., Sutherland, S. C., Feely, R. A., and Wanninkhof, R.: Decadal change of the surface water pCO_2 in the North Pacific: a synthesis of 35 years of observations, J. Geophys.

Res., 111, C07S05, doi:10.1029/2005JC003074, 2006.
Takahashi, T., Sutherland, S. C., Wanninkhof, R., Sweeney, C., Feely, R. A., Chipman, D. W., Hales, B., Friederich, G., Chavez, F., Sabine, C., Watson, A., Bakker, D. C. E., Schuster, U., Metzl, N., Yoshikawa-Inoue, H., Ishii, M., Midorikawa, T., Nojiri, Y., Körtzinger, A., Steinhoff, T., Hoppema, M., Olafsson, J., Arnarson, T. S., Tilbrook, B., Johannessen, T., Olsen, A., Bellerby, R., Wong, C. S., Delille, B., Bates, N. R., and de Bar, H. J. W.: Climatological mean and decadal change in surface ocean pCO_2 and net sea-air flux over global oceans, Deep-Sea Res. Pt. II, 56, 554–577, 2009.
Uppala, S. M., Kållberg, P. W., Simmons, A. J., Andrae, U., et al.: The ERA-40 re-analysis, Q. J. Roy. Meteor. Soc., 131, 2961–3012, 2005.
Wanninkhof, R.: Relationship between wind speed and gas exchange over the ocean, J. Geophys. Res., 97, 7373– 7382, 1992.

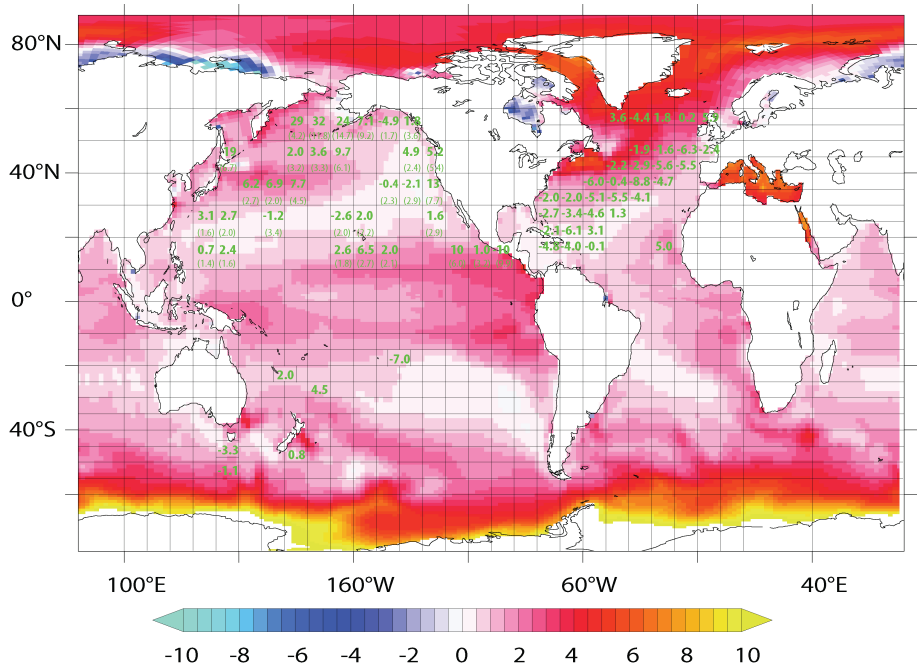

Fig. 1. Decadal trends in the annual mean of ΔpCO_2 over 1970–2000 (µatm decade^{-1}) computed from the annual mean of DIC, SST, Alkalinity and Salinity. The numbers in bold green letters indicate the decadal trends of ΔpCO_2 computed from Takahashi et al., (2006, 2009) assuming a 1.5 µatm yr^{-1} increase of the atmospheric CO_2 concentration over 1970–2000. The values in parenthesis indicate the uncertainty in the same unit. In boxes without parenthesis numbers, uncertainty ranges from 1 to 6 µatm decade^{-1}.

BGD
7, 745–764, 2010

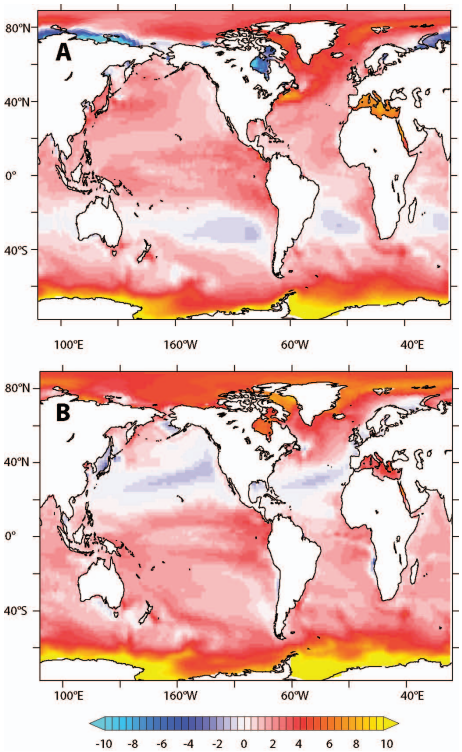

Fig. 2. (A) Decadal trends of ΔpCO_2 for February over 1970–2000 (μatm decade^{-1}) computed from the DIC, SST, Alkalinity and Salinity in February; **(B)** same as (A) but for August (i.e. computed from the DIC, SST, Alkalinity and Salinity in August).

BGD
7, 745–764, 2010

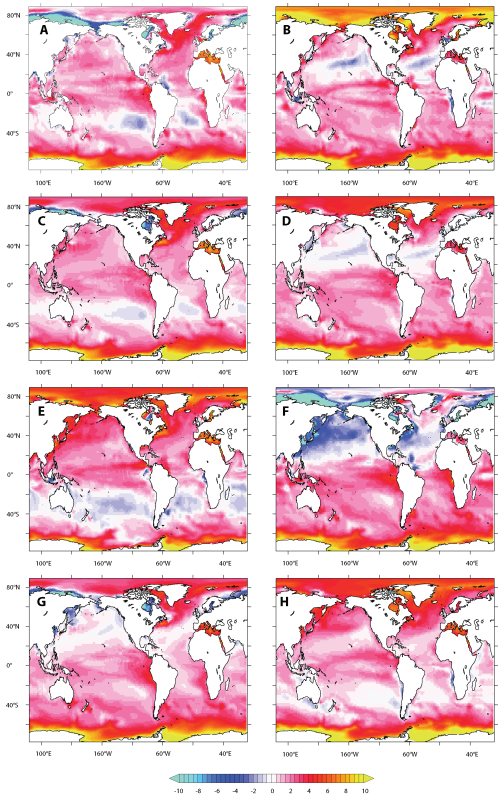

Fig. 3. **(A, *B*)** Decadal trends (μatm decade^{-1}) in February (*August*) ΔpCO_2 over 1970–2000 computed from the annual mean of Alkalinity and the seasonal DIC, SST and Salinity; **(C, D)** same as (A, B) but using the annual mean of Salinity and the seasonal Alkalinity, DIC and SST in the ΔpCO_2 calculation; **(E, F)** same as (A, B) but using the annual mean of DIC and the seasonal Alkalinity, SST, and Salinity; **(G, H)** same as (A, B) but using the annual mean of SST and the seasonal DIC, Salinity, and Alkalinity.

BGD
7, 745–764, 2010

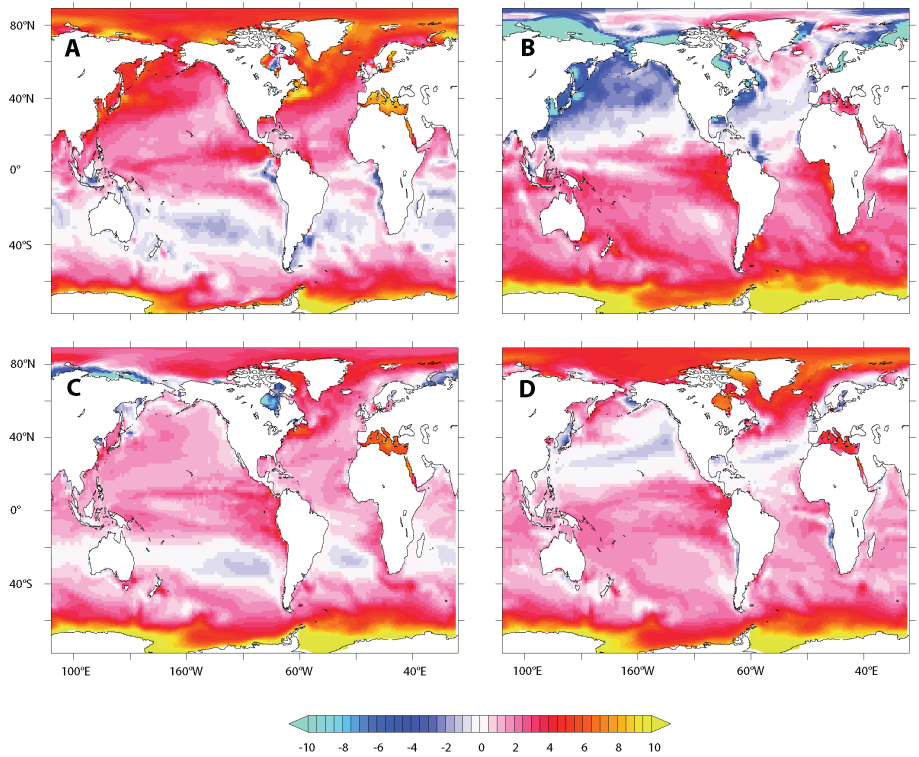

Fig. 4. (A, *B*) Decadal trends (µatm decade^{-1}) in February (*August*) ΔpCO_2 over 1970–2000 computed from the annual mean of DIC_{pre} and the seasonal SST, Alkalinity, Salinity and DIC_{ant}; **(C, D)** same as (A, B) but using the annual mean of the DIC_{ant} and the seasonal SST, Alkalinity, Salinity and DIC_{pre}.

BGD
7, 745–764, 2010

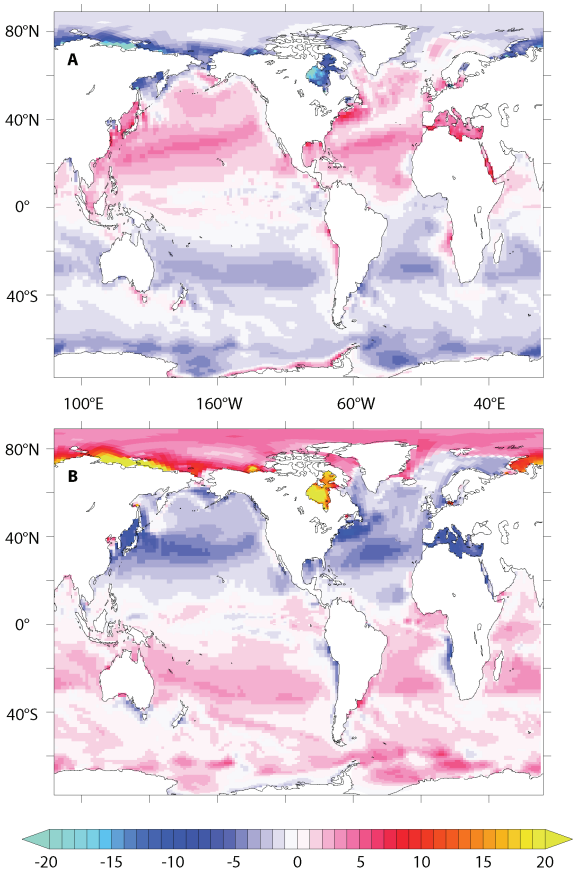

Fig. 5. (A) Difference (µatm) in 2000 between the mean anthropogenic ΔpCO_2 and the ΔpCO_2 computed from the boreal winter (February) trends only. **(B)** same as (A) but using the ΔpCO_2 computed from the boreal summer (August) trends instead of the winter trends.

BGD
7, 745–764, 2010